ANNALS OF GEOPHYSICS, 66, 2, Se213, 2023; doi:10.4401/ag-8825
OPEN ACCESS

Azimuthal Anisotropy of Receiver Functions in the Central South China Block and its Tectonic Implications

Yutao Shi[1], Yuan Gao[*,1], Ziqi Zhang[2], Yongqian Zhang[3], Guohui Li[1]

(1) Key Laboratory of Earthquake Prediction, Institute of Earthquake Forecasting, China Earthquake Administration, Beijing, 100036, China

(2) Department of Earth and Environmental Sciences, University of Rochester, Rochester, NY, USA

(3) China Deep Exploration Center-SinoProbe Center, China Geological Survey & Chinese Academy of Geological Sciences, Beijing 100037, China

Article history: received March 26, 2022; accepted November 14, 2022

Abstract

By the H-κ stacking of the receiver functions and the splitting of the Pms phases, using seismic data from the Regional Seismic Network and the Huanan Seismic Array, a high-resolution temporary seismic array deployed for 2 years in the study area. This study revealed the strong lateral heterogeneity in crustal structures in the central South China block. Crustal thickness reduces from northwest to southeast, with significant differences across the boundary of sub-blocks. The average crustal Vp/Vs ratio gradually increases from west to east, leading to high values in the coastal region, which suggests that the subduction of the Pacific plate has possibly caused the underplating of magma or the upwelling of upper mantle material. The crustal azimuthal anisotropy of the Dabie orogen and the Jiangnan orogen is generally consistent with the strike of the tectonic belt as well as with the orientation of the absolute plate movement. We suggest that the crustal azimuthal anisotropy of the orogen is related to the extension and deformation of the lithosphere. The anisotropy in the crust is close related to crustal deformation. The orientation in the crust and the upper mantle in the Cathaysia block are generally consistent with the orientation of the absolute plate motion, indicating that the azimuthal anisotropy of the Cathaysia block is related to lithospheric deformation and the under-invasion of upper mantle material.

Keywords: Azimuthal Crustal Anisotropy; Central South China Block; Crust Thickness; Vp/Vs ratio; Receiver function

1. Introduction

The South China block, located in the south of the Dabie orogen and east of the Tibetan Plateau, experienced a long term and multi-phase tectonic evolution, and finally formed the present unified tectonic pattern [Shu, 2012]. It is widely accepted that this dynamic tectonic evolution differs from the single oceanic plate tectonic processes

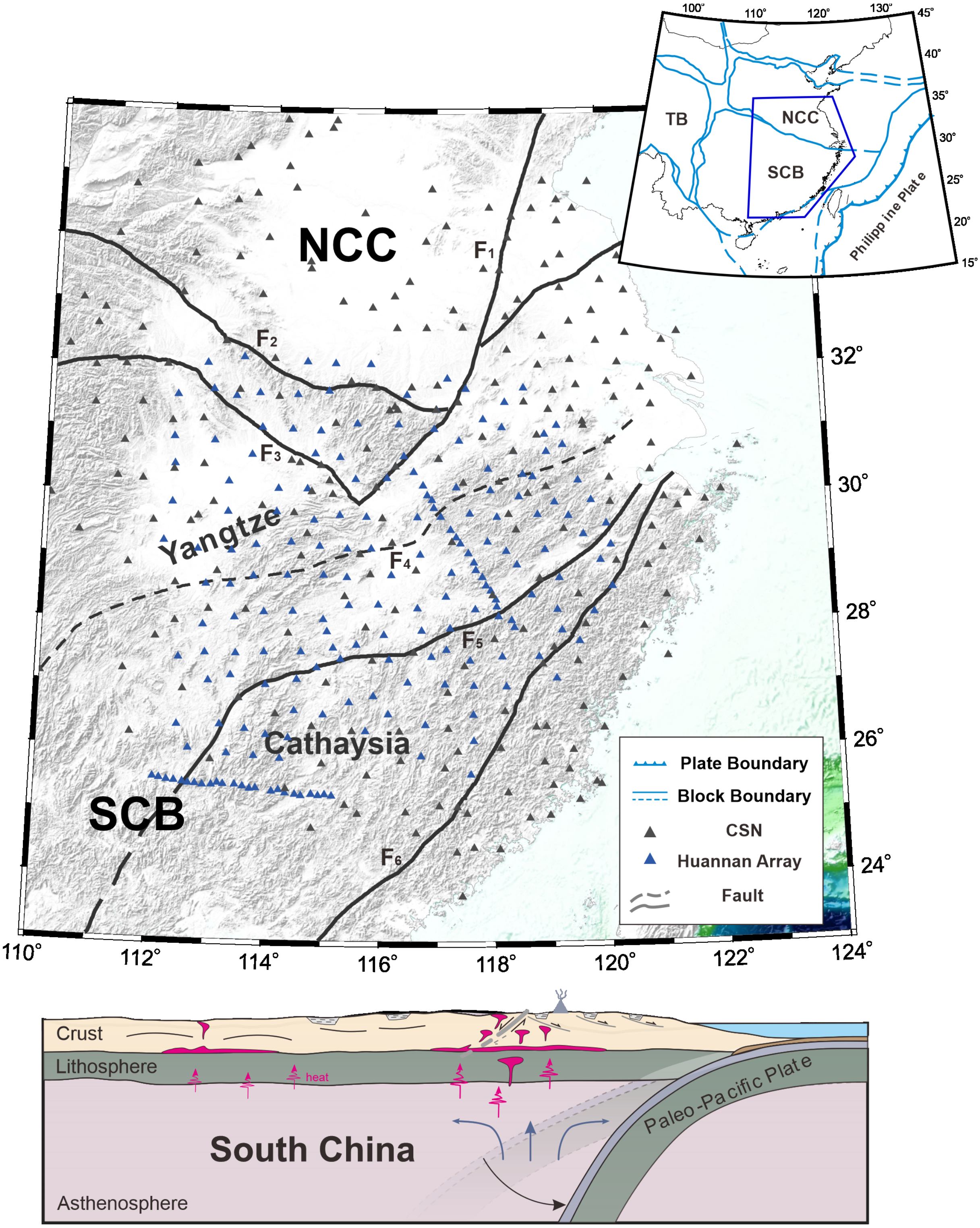

Figure 1. Distribution of seismic events, seismic stations and faults in the central South China block. Dark gray triangles and dark blue triangles represent the stations of the Regional Seismic Network and the Huanan Seismic Array used in this study, respectively. NCC: North China craton; SCB: South China block; DB: Dabie orogen; JN: Jiangnan orogen; F_1: Tanlu fault; F_2: Xinyang-Shucheng fault; F_3: Xiangfan-Guangji fault; F_4: The hidden fault for the north boundary of the Jiangnan orogen; F_5: Jiangshan-Shaoxing-Pingxiang fault zone; F_6: Zhenghe-Dapu fault. F_2 and F_3 are the north-south boundaries of Dabie orogen. F_4 and F_5 are the north-south boundaries of the Jiangnan orogen. The location of the study area is indicated by the blue frame in the inset plot at the top right corner. The picture below show the schematic model of the subduction of the Pacific plate revised after Zhang et al. [2021a].

and the continental plate tectonic evolution mechanism, presenting unique features with integral relative stability and independence of the internal sub-blocks in the South China block [Zhang et al., 2013].

The South China block was formed from the Neoproterozoic collision of the Cathaysia block and the Yangtze Craton, the suture of which is marked by the Jiangnan orogen, and is widely accepted to have collided with North China [Figure 1; Shu, 2012; Zhang et al., 2013]. The Yangtze Craton and the Cathaysia block have mainly been regarded as two unified geological units in most geodynamic studies, with less active tectonic faults and weak seismic activity [Zheng et al., 2013]. The South China block has undergone multi-stage regional scale tectonic and magmatic events during early Paleozoic and early Mesozoic, which resulted in different shapes and the properties of the lithosphere in the Yangtze Craton and the Cathaysia block [Lin et al., 2018].

Specifically, the Cathaysia block has experienced lithospheric thinning and delamination, whereas the Yangtze Craton has evolved into a relatively stable quasicraton [Shu, 2012]. Many studies have shown that the tectonic mechanism of the Yangtze Craton and the Cathaysia block have been affected by the compositions and multi-scale inhomogeneity of lithospheric structures [Ai et al., 2007; Zheng et al., 2008; Luo et al., 2012; Lv et al., 2016; Ding et al., 2017; Shahzad et al., 2021]. The North hidden fault zone and the Jiangshan-Shaoxing-Pingxiang fault are the boundaries of the Jiangnan orogen, which divided the South China block into the Yangtze Craton and the Cathaysia block [Shu et al., 2009; 2011; Zhang et al., 2013]. The Zhenghe-Dapu fault zone divides the Cathaysia block into the east and west sub-blocks [Xu et al., 2007; Zhang et al., 2014]. Geophysical observations revealed that there are obvious differences in lithosphere morphology, material composition and crustal thickness on both sides of the tectonic boundary faults [Charvet et al., 1996; Xiong et al., 2009; Zhao et al., 2015]. In recent years, there are extensive geophysical studies of lithospheric structure focusing on the deep tectonic and dynamic processes in the South China block [Xu et al., 2007; Wang et al., 2014; Sun et al., 2016; Luo et al., 2019]. The absence of adequate seismic station coverage and the limited coverage of seismic profile observation lead to the low knowledge and resolution of the lithospheric structure [Wang et al., 2000; Ye et al., 2019]. Consequently, there are still debates on the coupling relationship between sub-blocks in the South China block, and the structure of each block needs to be further investigated [Shu, 2012].

Receiver function is a robust and informative technique for studying crustal deformation and dynamic mechanisms. The estimation of the average crustal thickness and the Vp/Vs ratio by converted Pms phase receiver function can be used to understand the crustal structure [Zandt and Ammon, 1995]. In addition, receiver function has been proved to be also useful in anisotropy studies. The anisotropy of converted Pms phase receiver function is helpful to investigate the dynamic characteristics in the lithosphere [Vinnik et al., 1992; Sun et al., 2012; Wang et al., 2016; Kong et al., 2018; Zheng et al., 2018]. Study suggests that channelized plastic flow in the mid-lower crust can result in azimuthal anisotropy [Ko and Jung, 2015]. In order to achieve a better understanding of regional tectonic and magmatic processes, a high-resolution seismic array with 200 broadband seismic stations deployed in the central South China block, which covers the eastern Dabie orogen, Jiangnan orogen, middle and lower Yangtze Craton, and part of the Cathaysia block. This study collected seismic data recorded by the Regional Seismic Network and high-resolution seismic array to obtain the crustal structure and the anisotropic parameters using receiver function, and further analyze the lithospheric deformation and composition within the sub-block in the central South China block.

2. Data and methods

In this study, we used teleseismic events larger than *M*s5.5 recorded by 174 seismic stations from the Regional Seismic Network from January 1, 2012 to December 31, 2017. We also used additional data recorded by a high-resolution temporary seismic array, the Huanan Seismic Array, which includes 200 broadband seismic stations. The Huanan Seismic Array consisted of 100 seismic stations with STS-2.5 seismometer and Q330s recorder deployed by the Chinese Academy of Geological Sciences from September 2014 to July 2016, 40 seismic stations with Guralp-3T seismometer and Reftek-130 recorder deployed by the Peking University from October 2014 to July 2015, 20 seismic stations with Guralp-40T seismometer and Reftek-130 recorder deployed by the Nanjing University from September 2014 to December 2015, and 40 seismic stations with 30 Nanomatrics seismometers and 10 CZS-II seismometers deployed by the Institute of Earthquake forecasting, China Earthquake Administration from December 2014 to August 2016. The sampling frequency of all the waveform records is 100 samples per second. For receiver function analysis, we chose seismic events with clear initial motion and epicentral distance ranging from 30° to 90°. Qualified events used in the analysis have a good spatial coverage (Figure 2).

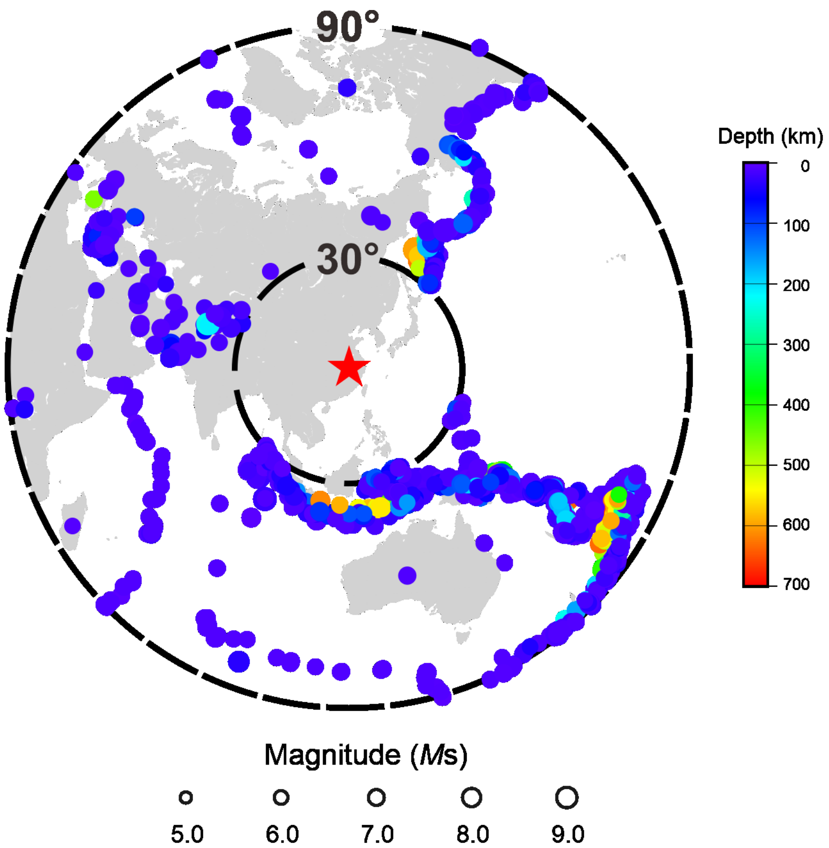

Figure 2. Earthquake distribution against epicentral distance used in this study. For a given event, the size of the circles is proportional to the magnitude (*Ms*), and the color of the circle corresponds to the focal depth. The circles labeled as 30° and 90° denote epicentral distances from the center of study area, which was marked as a red star.

The receiver function method is suitable for detecting the crustal composition and dynamic evolution of the crust [Ammon, 1991; Shen et al., 2014; Tian et al., 2014; Zhang et al., 2021a, b]. Trade-offs between H (crustal thickness) and κ (Vp/Vs ratio) can be circumvented by using the arrival times and the amplitudes of the conversion phase Pms and its multiples (PpPms, PpSms + PsPmsPs) from the Moho discontinuity [Zhu and Kanamori, 2000; Zandt and Ammon, 1995]. Assuming a horizontally stratified crustal layer and small velocity lateral variation in the study area, the crustal thickness and Vp/Vs ratio were obtained by H-κ scanning analysis of the P-wave receiver functions, which is based on a grid scanning method [Zhu and Kanamori, 2000; Gao and Liu, 2014]. In this study, the time-domain iterative deconvolution technique [Ligorria and Ammon, 1999] is employed to compute the P-wave receiver functions. A Gaussian low-pass filter with a Gaussian width factor of 5.0 Hz is utilized to further remove high-frequency noise. The original seismic records were bandpass filtered between 0.02 and 1.0 Hz to ensure robust receiver function calculations. The average crustal P-wave velocity is set to 6.1 km/s [Xiong et al., 2009]. The scanning ranges of crustal thickness and Vp/Vs ratio are 15 km-55 km and 1.65-1.95.

The phase Pms wave has the largest signal to noise ratio while the PpSms + PsPms wave has the smallest signal to noise ratio. Therefore, the weighting factors for the Pms and its multiples are 0.7, 0.2 and 0.1, respectively. These weighting factors are chosen to balance the contributions from the three phases [Zhu and Kanamori, 2000]. Figure 3 shows examples of determination of the crustal thickness and the Vp/Vs ratio by H-κ scanning from the stations SCH, YIY, DSXP and HJ11.

In isotropic media, the converted Pms phase has energy only on the radial component. However, in a horizontal transverse isotropic (HTI) medium, the converted Pms phase also has energy on the tangential component [Nagaya et al., 2008; Liu and Niu, 2012]. For a single-layer weak anisotropy model, the relationship between the arrival time of PmS phase and the earthquake back azimuth can be approximately expressed as [Rumpker et al., 2014]

$$t = t_0 + \Delta t = t_0 - \frac{\delta t}{2}\cos\left[2\left(\varphi - \varphi_f\right)\right] \tag{1}$$

where t_0 is the arrival time of Pms in the isotropic case, δt denotes the azimuthal moveout with respect to t_0, φ is the back-azimuth of the receiver functions, and φ_f is the crustal fast polarization orientation.

In this study, the splitting parameters were obtained by fitting the PmS arrival times relative to the direct P-wave using Equation (1) based on a non-linear least-squares fitting procedure [Kong et al., 2016; 2018] and by the grid-searching to improve the reliability of the resulting anisotropy parameters [Rumpker et al., 2014]. This approach has been widely adopted in investigating crustal anisotropy [Zheng et al., 2018; 2019]. An example can be found in Figure 3.

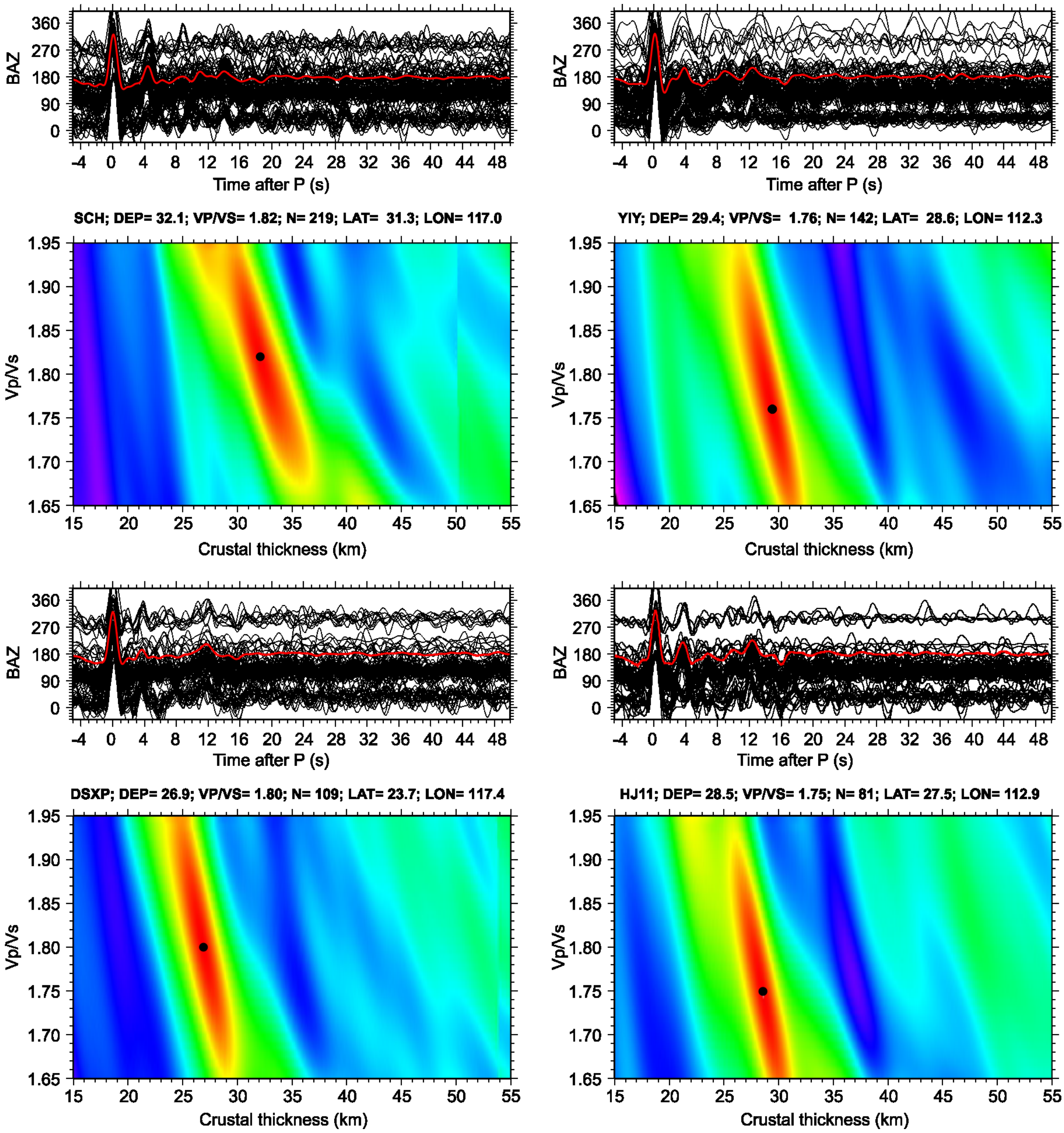

Figure 3. Receiver function traces and H-κ scanning analysis of station SCH, YIY, DSXP and HJ11. Top panel for each station shows receiver function traces plotted against back azimuth (black) and the stacked average (red) of all traces; bottom panel for each station shows the grid search for crustal thickness and Vp/Vs ratio calculation.

Figure 4 shows an example of crustal anisotropy measured at temporary stations HJ28 and ah202, and at two Regional Seismic Network stations BZY and HAJF using the converted Pms phase receiver function.

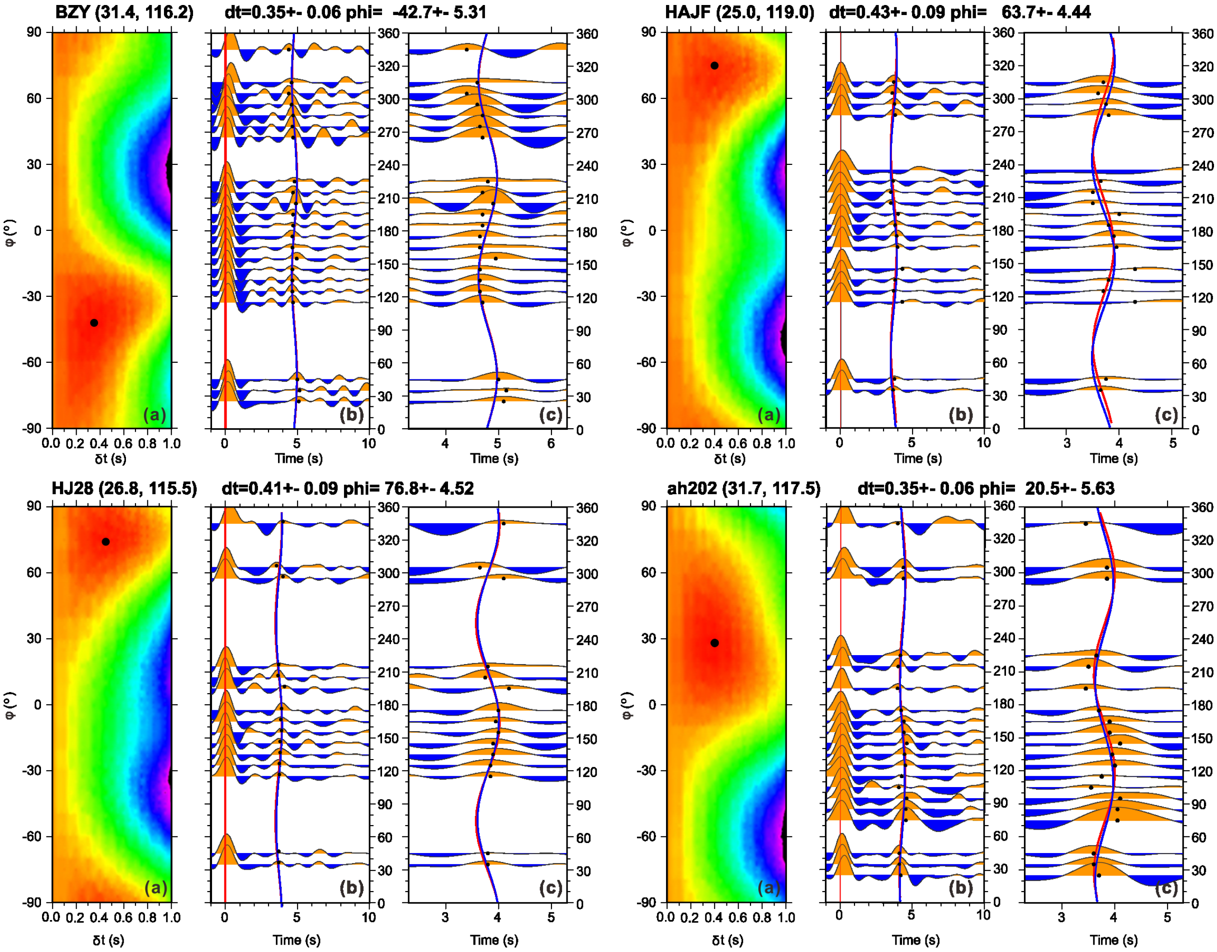

Figure 4. Measurements of crustal anisotropy at the stations BZY, HAJF, HJ28 and ah202. (a) The measurements of the crustal anisotropy beneath each station. The energy diagram illustrating the stacked energy of the all the candidate pairs of radial receiver functions from the grid search for splitting parameters φ_f and δt. The best fitting pair of splitting parameters is marked by a black dot. (b and c) Radial receiver function traces against back azimuth. The black dot is the maximum amplitude of the Pms seismic phase. The red and blue lines represent the optimal curve calculated based on equation (1) of Kong et al. [2016] using the optimal pair of anisotropy parameters from the stacking and fitting the Pms moveout, respectively. (b) is enlarged from (c) to show the Pms seismic phase arrival only.

3. Crustal thickness and velocity ratio

In this study, the crustal thickness and the Vp/Vs ratio distributions under 308 stations were obtained by H-κ scanning analysis (Table S1 in the supporting information, Figure 5), including the 140 stations of the Regional Seismic Network and the 168 stations of the Huanan Seismic Array. Crustal thickness and Vp/Vs ratio range from 26 km to 38 km and 1.65 to 1.88, respectively, with average values of 32 km and 1.75 in the central South China block. These results are in agreement with the previous studies at the South China block and its surrounding areas [Song et al., 2017; Ye et al., 2019; Guo et al., 2019; Zhang et al., 2021a, b].

Our results show that the crust is thicker to the northwest and thinner to the southeast of the central South China block, decreasing towards the coast (Figure 5a). The Dabie orogen is a tectonic convergence zone between the North China Craton and Yangtze Craton. The crustal thickness of the Dabie orogen and the Hefei basin ranges from 32 km to 38 km, which is consistent with results obtained by the deep seismic soundings [Wang et al., 1997]. The Tanlu fault is a large strike-slip fault zone across the Yangtze Craton, the North China Craton, and the Dabie orogen, which has experienced multiple tectonic movements. The intense variation of the crustal thickness on its both sides indicates that the Moho is obviously dislocated by the Tanlu fault zone, which is also supported by results provided by deep seismic reflection profile and P-wave velocity imaging [Gao et al., 2004; Chen et al., 2008; Sun and Kennett, 2016]. Crustal thickness of the middle and lower Yangtze Craton ranges from 30 km to 36 km. In this region, the Jianghan and Subei basin has a thinner crust, while the internal basin corresponds to a thicker crust. Ambient seismic noise imaging also revealed that the depth of the Moho has an evident discontinuity in the middle and lower Yangtze Craton [Shi et al., 2013]. Our measurements confirm that the fault of the southern margin of the Dabie orogen and the Tanlu fault are the crustal thinning boundaries of the South China block [Li et al., 2018]. Crustal thickness of the Cathaysia block is quite small, ranging from 26 km to 32 km, with small variations. Our results suggest that the lithosphere was trough delamination and the crustal thickness decreases from continent to coast under the tectonic evolution of the Cathaysia block.

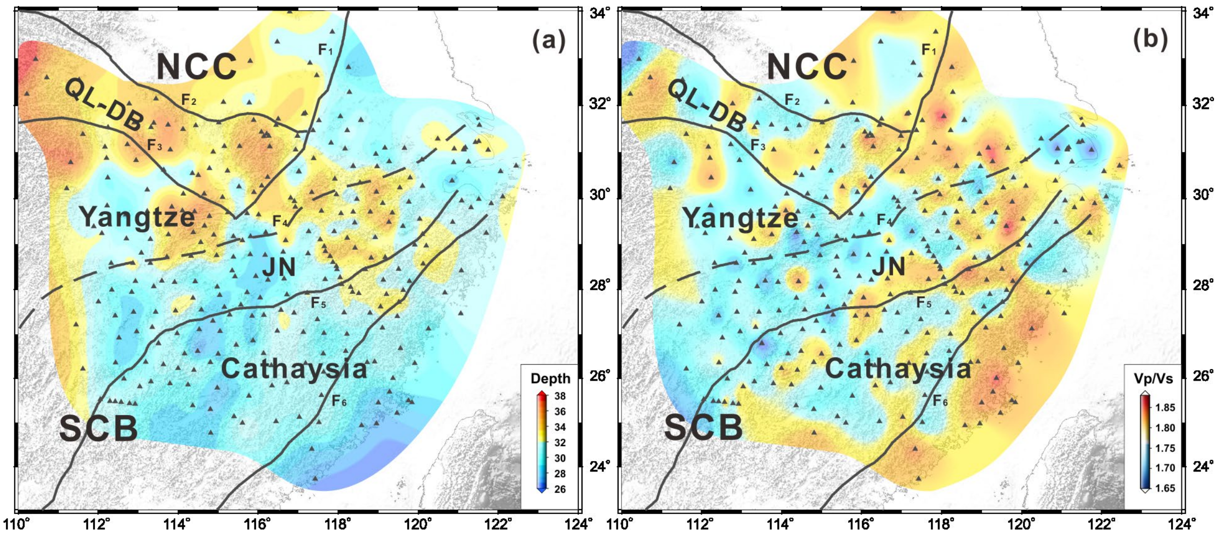

Figure 5. The distribution of crustal thickness (a) and Vp/Vs ratio (b) obtained by H-κ scanning analysis of receiver function in the study area. The black triangles represent the location of seismic stations.

In the central South China block, the Vp/Vs ratio shows complicated spatial variation patterns. Overall, the Vp/Vs ratio is lower in the western and higher in the southeastern of the study area (Figure 5b). Average crustal Vp/Vs ratio is an important factor for indicating the composition of the crustal material [Ji et al., 2013]. Our results reveal low crustal Vp/Vs ratio along the Dabie and Jiangnan orogen. In addition, high crustal Vp/Vs ratio with changes is observed at the Tanlu fault zone and its surrounding area. The deep-seated faults likely served as channels for the rising magmas, which allowed more mafic magmatic material with high Vp/Vs ratio to be intruded into the crust near the fault zone [Wan and Zhao, 2012]. Our results revealed that the tectonic activity of the fault zone has led to the partial melting of the upper mantle and the upwelling of the asthenosphere materials. The Cathaysia block is a part of the low velocity zone of the west Pacific in Southeast Asia. In this region, the lithosphere was transformed by the uplift of the asthenosphere and shows multi-period and intense magmatism by the extensive distribution of Mesozoic volcanic rocks and granites [Li and Li., 2007; Huang et al., 2010; Deng et al., 2019]. Our results show that the average crustal Vp/Vs ratio increases from continent to coast in the Cathaysia block. As an important sub-block boundary zone of the Cathaysia block [Shu et al., 2009; 2011; Zhang et al., 2014], the Vp/Vs ratio on the east side of the Zhenghe-Dapu fault is larger than on its west side. These results suggest that the intensity of magmatic activity [Zhou and Li, 2000, Zhou et al., 2000; 2006, Shu et al., 2009, Li et al., 2012; Li et al., 2014a] gradually increased from the continent to the coast within the Cathaysia block, and verify that the bottom erosion of mafic rocks led to the increase of the velocity ratio [Zhou and Li, 2000; Shen et al., 2000].

The spatial distribution of the crustal thickness and the average Vp/Vs ratio in the central South China block is relevant to the crustal evolution since the Mesozoic [Shu et al., 2011]. Under the compression of surrounding blocks, strong nappe structure was formed around the sub-block boundary zone, which possibly caused the observed increasing crustal thickness and decreasing Vp/Vs ratio from the east to the west of the South China block. These results reveal that the Tanlu fault zone cuts the Moho and presents high Vp/Vs ratio, and has experienced complicated geological tectonic evolution, resulting in an unstable crustal structure during the block collision of the South China block and the North China Craton [Shi et al., 2013]. Since the Mesozoic, due to the horizontal movement of asthenosphere material, the Cathaysia block has experienced magma intrusion, volcanic activity and crustal magmatic underplating [Zhou and Li, 2000; Sun et al., 2016]. The lithosphere was destroyed and uplift into the crust where with high Vp/Vs ratio.

4. Estimation of crustal anisotropy

In this study, the crustal anisotropy of 105 stations in total were well-determined with an adequate back azimuth coverage for measuring crustal anisotropy by visual checking, including the 72 stations of the Regional Seismic Network and the 33 stations of the Huanan Seismic Array (Table S2 in the supporting information, Figure 6). The orientation of crustal anisotropy displays clear spatial patterns with little variation. The time delay ranges from 0.16 s to 0.62 s in the entire region, with an average of (0.34 ± 0.08) s, which is slightly larger than the crustal anisotropy in the North China [Yang et al., 2018; Zheng et al., 2019]. Previous studies have shown that the anisotropy due to propagation in the upper crust generally contributes from 0.04 s to 0.2 s to the shear wave splitting [Savage, 1999; Kaviris et al., 2017]. The time delay measurements are larger than these values, indicating that the observed seismic anisotropy is probably due to propagation to the whole crust, which is mainly caused by minerals aligned during ductile flow of the lower crust, corresponding to the deformation of structure among each block in the study area.

According to the local tectonic features and obtained the crustal thickness and Vp/Vs ratio, the central South China block can be divided into six sub-regions in this study: Hefei basin in the southern North China Craton (Zone A), East Dabie orogen (Zone B), middle and lower Yangtze Craton (Zone C), East Jiangnan orogen (Zone D) and east and west Cathaysia block (Zone E and Zone F) (Figure 6).

The Hefei basin (Zone A), a large-scale continental depositional basin, sits around the juncture of the North China Craton and the Yangtze Craton, linking the Dabie orogen and the Tanlu fault, that controlled its formation and evolution [Lu et al., 2002]. In this study, the orientations of crustal anisotropy are NW and NNW at stations located at the Hefei basin and its surrounding area, which are consistent with polarization direction of upper mantle seismic anisotropy, as revealed by the measurements of XKS (SKS/PKS/SKKS) splitting [Wu et al., 2012]. The measured mean time delay of crust is (0.29 ± 0.06) s in this study, which is slightly larger than the crustal anisotropy by the local shear wave splitting in the middle North China Craton [Wu et al., 2007; Shi et al., 2015]. This study suggested that the crustal anisotropy originates from the deformation difference between the lithosphere and the asthenosphere in the Hefei basin.

The Dabie orogen (Zone B) was formed by continent-continent collision between the North China block and the South China block formed after the Indosinian. The petrological features of granites indicated the middle-lower crust ductile flow beneath the Dabie orogen [Li et al., 2014b; Yu et al., 2016]. In this study, the measured NW orientations of crustal anisotropy at most stations, which is basically parallel to the tectonic strike of the orogen and the absolute plate motion orientation (Figure 6). The mean time delay is (0.38 ± 0.07) s, which is in agreement with previous studies in the area [Huang et al., 2013, Liu et al. 2019]. The orientation of the crustal anisotropy is basically consistent with upper mantle anisotropy measured by XKS splitting. The mean time delay is lower than the one attributed to upper mantle anisotropy, which is 1.3-2.2 s [Shi et al., 2013; Zhao et al., 2013].

The middle and lower Yangtze Craton (Zone C) is placed in complicated tectonic systems among multiple blocks, including the Dabie orogen, the Jiangnan orogen and the Tanlu fault belt. The orientations of crustal anisotropy at stations in Zone C show zoning features with the mean time delay equal to (0.38 ± 0.08) s. The middle Yangtze Craton is trapped between the Dabie and Jiangnan orogen, mainly affected by the thrust nappe of the Dabie orogen, with NNW and NEE strike of faults [Xu and Gao, 2015]. The crustal anisotropy at four stations (HUR, JME, JYU and SSH) located in the middle Yangtze Craton shows NNW orientation, consistent with the NNW strike of the local tectonic fault. The mean time delay for these stations is (0.36 ± 0.08) s. During the collision between the Yangtze Craton and the North China Craton along the Tanlu fault zone, the nappe structure and fold deformation with NE-ENE orientation were formed in the lower Yangtze Craton [Xu and Gao, 2015]. The measurements of crustal anisotropy in this study area reveal NE to ENE with a mean time delay of (0.39 ± 0.07) s, which are consistent with previous measurements in the middle Yangtze Craton [Huang et al., 2013]. Therefore, we suggest that the whole crustal anisotropy reflects folding deformation of the crust in the middle Yangtze Craton. The orientations of anisotropy at stations JGS, JIJ, DUC, and HN34 are nearly EW oriented at the intersection of the Dabie orogen and the Tanlu fault,

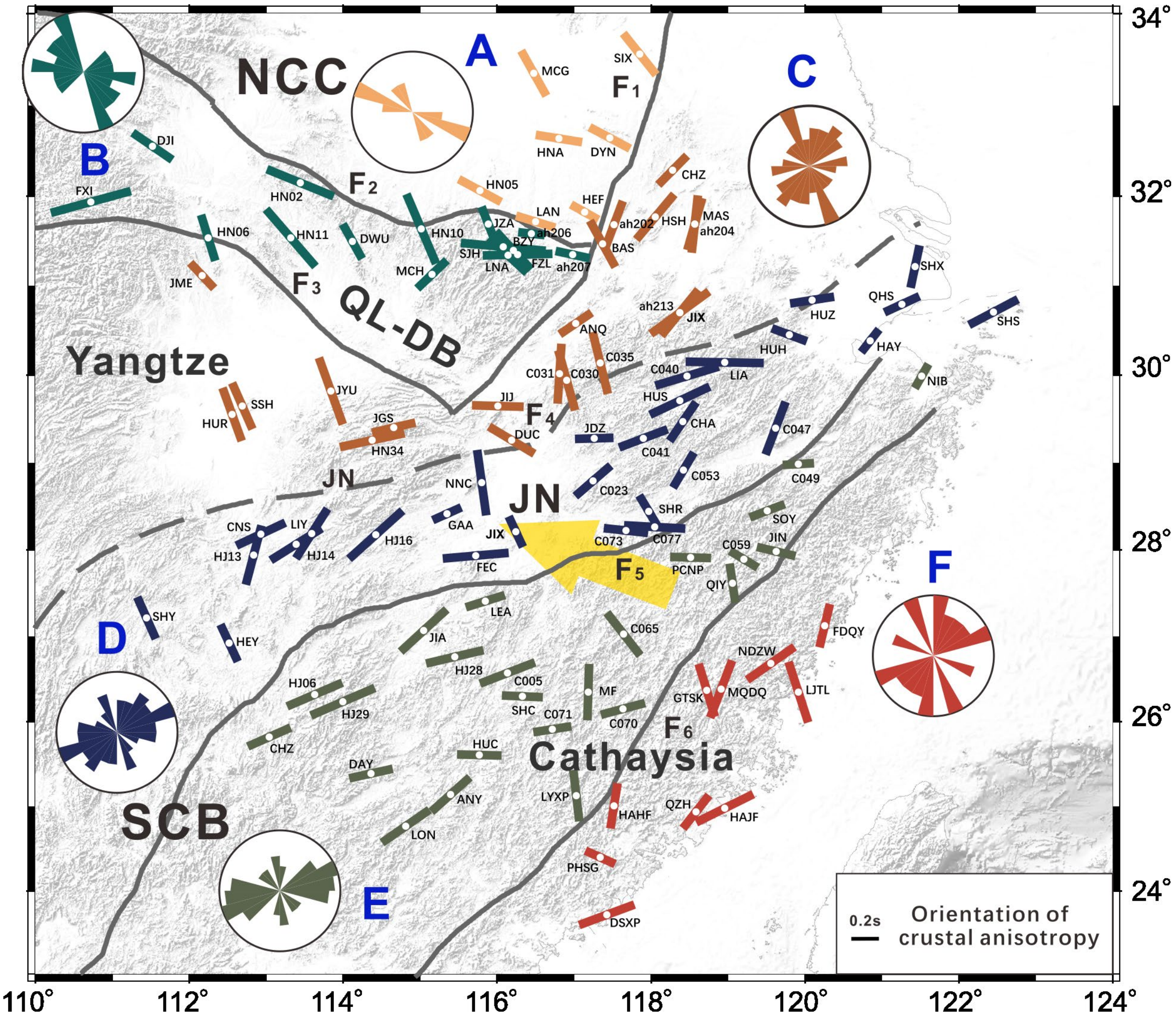

Figure 6. Crustal anisotropy measurements in the central South China block. The orientation and length of the color lines represent the fast share wave polarization direction and time delay at each station. The rose diagrams presents the anisotropy direction of each region: A, Hefei Basin; B, Dabie orogen; C, Yangtze Craton; D, Jiangnan orogen; E and F, East and West Cathaysia block. The yellow arrow indicate the absolute plate motion directions [Zhao et al., 2013].

which is consistent with the geological folding and the strike of the local faults [Xiao et al., 2000]. The mean time delay is (0.37 ± 0.08) s. Compared with the upper mantle anisotropy [Wu et al., 2012], the considerable difference reveals the different tectonic movement between the crust and the upper mantle in the middle and lower Yangtze Craton (Zone B).

The crustal anisotropy at stations to the east of the Jiangnan orogen (Zone D) is related to NE oriented with mean time delay of (0.34 ± 0.07) s. The orientation of crustal anisotropy is consistent with the trend of the orogen. Previous XKS splitting analysis obtained the mean upper mantle anisotropy polarization of NE orientation and the time delay of about 1.0 s in the eastern Jiangnan orogen [Shi et al., 2013; Wang et al., 2014]. Based on the coherence of crustal and upper mantle anisotropy, we infer that the anisotropy is driven by the east-west extensional deformation of the whole lithosphere in the Jiangnan orogen.

The Zhenghe-Dapu fault is an important suture zone in the Cathaysia block, which can be divided into two terranes, the west (Zone E) and the east (Zone F) Cathaysia blocks [Zhang et al., 2014; Lin et al., 2018]. Our measurements show little contrast in the fast orientations between the west and the east Cathaysia blocks. The measurements of crustal anisotropy at the majority of the stations in the west Cathaysia block are approximately ENE oriented, which is oblique to the orientation of the absolute plate movement with small angle (Figure 6). The mean time delay of whole crust is (0.32 ± 0.08) s. The orientation of the crustal anisotropy on the east Cathaysia block is NE, which is basically consistent with the fault strike. The mean time delay is (0.37 ± 0.08) s, which is approximately the same as in the west Cathaysia block. Previous studies have shown that the orientation of XKS splitting is NE or ENE in the Cathaysia block [Wu et al., 2007; Huang et al., 2011; Zhao et al., 2013; Yang et al., 2019], which is generally in agreement with whole crustal anisotropy from this study. Coupling relationship between the crust and mantle is closely related to dynamic processes in the lithosphere [Flesch et al., 2005; Wang et al., 2008]. The orientation of the crustal and upper mantle anisotropy is slightly different from the APM direction in study area (Figure 6). Therefore, this study suggests that the lithosphere has experienced complex deformations during different geological periods beneath the South China block from the subduction of the Pacific plate.

5. Discussions and conclusions

The South China block is a major continental block in East Asia, which is formed by multi-phase plate and intracontinental tectonics, showing unique crustal structure and geodynamic features resulting from geodynamic evolution process. Based on the high-resolution seismic network, this study reveals the regional crustal structure in the central South China block. The results show that the crustal thickness decreases from west to southeast, while the average Vp/Vs ratio increases from west to southeast. The variation of the crustal thickness is concentrated at tectonic boundaries of sub-blocks, which is mainly controlled by regional tectonic and crustal movement among the sub-blocks. The high Vp/Vs ratio of the coastal area obtained by this study suggests that the subduction of the Pacific plate caused the underplating of the mantle-derived magmas and the upwelling of the upper mantle in the central South China block [Lin et al., 2019].

Affected by the tectonic confinement of the surrounding plates, orogens and faults, the complex crustal anisotropic structure has evolved inside the South China block. The spatial distribution of the crustal anisotropy recovered by receiver function showed distinct lateral variations of the orientation in different tectonic blocks. This result reveals intense deformation and apparent difference of the crustal structure within the central South China block. Based on the complicated spatial distribution of crustal anisotropy in the Yangtze block, there are notable variations of tectonic evolution in the middle and lower Yangtze Craton, which are related to the regional structures and interior orogens. The orientation of crustal anisotropy is the geological response of the strike of faulting and of the fold structures. In the Yangtze Craton, the difference of crustal and upper mantle anisotropy indicates the existence of a crust-mantle decoupling mechanism under multi-phase structural features and evolution. In the Cathaysia block, the orientations of anisotropy in the crust and upper mantle are basically consistent with the orientation of the absolute plate motion, which supports crust-mantle coupling mechanism and the vertically coherent deformation of the coupled lithosphere. The orientations of anisotropy are consistent with the orientation of the absolute plate movement also in the Dabie and Jiangnan orogen, indicating the dislocation creep and flow and the vertical coupling in the lithosphere

As the crustal thinning boundary of the continental margin of South China block, different sides of the Tanlu fault show notably different crustal anisotropy features. Similarly, as the boundary of crustal Vp/Vs ratio, the crustal anisotropy also shows evident variation across the Zhenghe-Dapu fault. Therefore, this study suggests that seismic anisotropy is closely associated with the variation of the crustal structure.

Acknowledgements. We would like to thank the Data Management Center of the China National Seismic Network at Institute of Geophysics, China Earthquake Administration (SEISDMC, http://dx.doi.org/10.7914/SN/CB). We would also like to thank Professor Stephen Shangxing Gao (Missouri University of Science & Technology) for providing the computational program for H-k stacking and RF anisotropy and Prof. Qiusheng Li (Institute of Geology, CAGS) for providing the wave data of Huanan Seismic Array. This work was supported by the NSFC Project (41604038, 42074099, 41774113), and China Geological Survey (12120114067701).

References

Ai, Y., Q. Chen, F. Zeng, X. Hong and W Ye (2007). The crust and upper mantle structure beneath southeastern China, Earth. Planet. Sci. Lett. 260, 3, 549-563.

Ammon, C. J (1991). The isolation of receiver effects from teleseismic P waveforms, Bull. Seismol. Soc. Am. 81, 2504-2510.

Charvet, J., L. Shu, Y. Shi, L. Guo and M. Faure (1996). The building of South China: Collision of Yangzi and Cathaysia blocks, problems and tentative answers, J. Asian Earth Sci., 13, 3-5, 223-235.

Chen, L., T. Wang, L. Zhao and T. Zheng (2008). Distinct lateral variation of lithospheric thickness in the northeastern North China Craton, Earth Planet. Sci. Lett., 267, 56-68.

Deng, Y., J. Li, T. Peng, Q. Ma, X. Song, X. Sun, Y. Shen and W. Fan (2019). Lithospheric structure in the Cathaysia block (South China) and its implication for the Late Mesozoic magmatism, Phys. Earth Planet. Inter., 291, 24-34.

Ding, W., Y. Fu, Y. Gao, W. Liao, Y. He, Y. Cai and X. Shen (2017). Phase velocity tomography of Rayleigh in Qinling-Dabie and its adjacent areas using ambient seismic noise, Chinese J. Geophys. (in Chinese), 60, 8, 2959-2968.

Flesch, L. M., W. E. Holt, P. G. Silver, M. Stephenson, C. Wang and W. W. Chan (2005). Constraining the extent of crust-mantle coupling in central Asia using GPS, geologic, and shear wave splitting data, Earth Planet. Sci. Lett., 238, 1-2, 248-268.

Gao, R., S. Dong, R. He, X. Liu, Q. Li, Y. Guan, J. Bai, P. Li, D. Huang, G. Qian, Z. Kuang and S. Li (2004). Subduction process of the Yangtze continental blockfrom Moho reflection image, South China, Earth Sci. Front. (in Chinese), 11, 3, 43-49.

Gao, S. S. and K. H. Liu (2014). Mantle transition zone discontinuities beneath the contiguous United States., J. Geophys. Res., 119, 6452-6468.

Guo, L., R. Gao, L. Shi, Z. Huang and Y. Ma (2019). Crustal thickness and Poisson's ratios in South China revealed by joint inversion of receiver function and gravity data, Earth Planet. Sci. Lett., 510, 142-152.

Huang, H., M. Xu, L. Wang, Z. Huang and P. Wang (2013). Distinct lateral variations of upper mantle anisotropy beneath eastern China revealed by shear-wave splitting, Geochem. Geophys. Geosyst., 14, 6, 1842-1855.

Huang, Z., L. Wang, D. Zhao, N. Mia and M. Xu (2011). Seismic anisotropy and mantle dynamics beneath China, Earth Planet. Sci. Lett., 306, 105-117.

Huang, Z., L. Wang, D. Zhao, M. Xu, N. Mi, D. Yu, H. Li and C. Li (2010). Upper mantle structure and dynamics beneath Southeast China., Phys. Earth Planet. Inter., 182, 161-169.

Ji, S., T. Shao, K. Michibayashi, C. Long, Q. Wang, Y. Kondo, W. Zhao, H. Wang and M. H. Salisbury (2013). A new calibration of seismic velocities, anisotropy, fabrics, and elastic moduli of amphibole rich rocks, J. Geophys. Res., 118, 4699-4728.

Kaviris, G., I., V. Spingos, P. Kapetanidis, N. Papadimitriou and K. M. Voulgaris (2017). Upper crust seismic anisotropy study and temporal variations of shear-wave splitting parameters in the Western Gulf of Corinth (Greece) during 2013, Phys. Earth Planet. Inter., 269, 148-164, doi: 10.1016/j.pepi.2017.06.006.

Ko, B. and H. Jung (2015). Crystal preferred orientation of an amphibole experimentally deformed by simple shear, Nat. Commun., 6, 6586.

Kong, F., S. S. Gao, K. H. Liu, J. Song, W. Ding, Y. Fang, A. Ruan and J. Li (2018). Receiver function investigations of seismic anisotropy layering beneath Southern California., J. Geophys. Res., 123, 10,672-10,683.

Kong, F., J. Wu, K. H. Liu and S. S. Gao (2016). Crustal anisotropy and ductile flow beneath the eastern Tibetan Plateau and adjacent areas, Earth Planet. Sci. Lett., 442, 72-79.

Li, H., X. Song, Q. Lu, X. Yang, Y. Deng, L. Ouyang, J. Li, X. Li and G. Jiang (2018). Seismic imaging of lithosphere structure and upper mantle deformation beneath east-central China and their tectonic implications, J. Geophys. Res., 123, 2856-2870.

Li, J., Y. Zhang, S. Dong and S. T. Johnston (2014a). Cretaceous tectonic evolution of South China: a preliminary synthesis, Earth Sci. Rev., 134, 98-136.

Li, S., S. Wang, S. Guo, Y. Xiao, Y. Liu, S. Liu, Y. He and J. Liu (2014b). Geochronology and geochemistry of leucogranites from the southeast margin of the North China Block: Origin and migration, Gondwana Res., 26, 3-4, 1111-1128.

Li, Z. and X. Li (2007). Formation of the 1300-km-wide intracontinental orogen and postorogenic magmatic province in Mesozoic South China: a flat-slab subduction model, Geology, 35, 179-182.

Ligorria, J. P. and C. J. Ammon (1999). Iterative deconvolution and receiver-function estimation, Bull. Seismol. Soc. Am., 89, 5, 1395-1400.

Lin, J., Y. Xu, Z. Sun, Z. Zhou (2019). Mantle upwelling beneath the South China Sea and links to surrounding subduction systems, National Sci. Rev., 6, 5, 877-881.

Lin, S., G. Xing, W. D. Donald, C. Yin, M. Wu, L. Li, Y. Jiang and Z. Chen (2018). Appalachian-style multi-terrane Wilson cycle model for the assembly of South China, Geology, 46, 4, 319-322.

Liu, H. and F. Niu (2012). Estimating crustal seismic anisotropy with a joint analysis of radial and transverse receiver function data, Geophys. J. Int., 188, 144-164.

Liu, Y., Y. Sun and J. Zhang (2019). Crustal structure and anisotropy beneath the Anhui province and its surroundings revealed by teleseismic receiver functions, Progress in Geophysics (in Chinese), 34, 2, 0442-0453.

Lu, G., G. Zhu, X. Li, D. Wang, C. Song and G. Liu (2002). A relationship between the Tan-Lu faulted belt and the petroleum geology of the Hefei basin, Petrol. Geol. Exp. (in Chinese), 24, 3, 216-222.

Luo, S., H. Yao, Q. Li, W. Wang, K. Wan, Y. Meng and B. Liu (2019). High-resolution 3D crustal S-wave velocity structure of the Middle-Lower Yangtze River Metallogenic Belt and implications for its deep geodynamic setting, Sci. China Earth Sci., 62, 1361-1378.

Luo, Y., Y. Xu and Y. Yang (2012). Crustal structure beneath the Dabie orogenic belt from ambient noise tomography, Earth Planet Sci Lett., 313-314, 12-22.

Lv, J., Z. Xie, Y. Zheng, X. Zha, R. Hu and X. Zeng (2016). Rayleigh wave phase velocities of South China block and its adjacent areas, Sci. China Earth Sci., 59, 2165-2178.

Nagaya, M., H. Oda, H. Akazawa and M. Ishise (2008). Receiver functions of seismic waves in layered anisotropic media: application to the estimate of seismic anisotropy, Bull. Seism. Soc. Am., 98, 2990-3006.

Rumpker, G., A. Kaviani and K. Latifi (2014). Ps-splitting analysis for multilayered anisotropic media by azimuthal stacking and layer stripping, Geophys. J. Int., 199, 146-163.

Savage, M. K (1999). Seismic anisotropy and mantle deformation: What have we learned from shear wave splitting? Rev. Geophys., 37, 1, 65.

Shahzad, S. M., J. Liu, Y. Sun and C. Li (2021). Crustal structure and deformation in southeastern China revealed by receiver functions, J. Asian Earth Sci., 221, 104937.

Shen, W., H. Ling, W., Li and D. Wang (2000). Crust evolution in Southeast China: evidence from Nd model ages of granitoids, Sci. China Earth Sci., 43, 1, 36-49.

Shen, X., Y. Zhou, Y. Zhang, X. Mei, X. Guo, X. Liu and M. Qin (2014). Receiver function structures beneath the deep large faults in the NEern margin of the Tibetan Plateau, Tectonophysics, 610, 63-73.

Shi, D., Q. Lv, W. Xu, J. Yan, J. Zhao, S. Dong and Y. Chang (2013). Crustal structure beneath the Middle-Lower Yangtze metallogenic belt in East China: Constraints from passive source seismic experiment on the Mesozoic intra-continental mineralization, Tectonophysics, 606, 48-60.

Shi, Y., Y. Gao and H. Jin (2015). The shear-wave splitting in the crust and the upper mantle around the Bohai Sea, North China, J. Asian Earth Sci., 111, 505-516.

Shu, L. 2012. An analysis of principal features of tectonic evolution in South China Block, Geol. Bull. China (in Chinese), 31, 7, 1035-1053.

Shu, L., M. Faure, J. Yu and B. Jahn (2011). Geochronological and geochemical features of the Cathaysia block (South China): new evidence for the Neoproterozoic breakup of Rodinia. Precambrian Research, 187, 263-276.

Shu, L., X. Zhou, P. Deng, B. Wang, S. Jiang, J. Yu and X. Zhao (2009). Mesozoic tectonic evolution of the Southeast China Block: new insights from basin analysis, J. Asian Earth Sci., 34, 3, 376-391.

Song, P., X. Zhang, Y. Liu and J. Teng (2017). Moho imaging based on receiver function analysis with teleseismic wave field reconstruction: Application to South China, Tectonophysics, 718, 118-131.

Sun, W. and B. L. N. Kennett (2016). Uppermost mantle P wave speed structure beneath eastern China and its surroundings, Tectonophysics, 683, 12-26.

Sun, Y., F. Niu, H. Liu, Y. Chen and J. Liu (2012). Crustal structure and deformation of the SE Tibetan plateau revealed by receiver function data: Seismic evidence for a lower crustal flow beneath the plateau, Earth Planet. Sci. Lett., 349-350, 186-197.

Tian, X., Z. Liu, S. Si and Z. Zhang (2014). The crustal thickness of NE Tibet and its implication for crustal shortening, Tectonophysics, 634, 198-207.

Vinnik, L., L. Makeyeva, A. Milev and A. Yu. Usenko (1992). Global Patterns of azimuthal anisotropy and deformation in the continental mantle, Geophys. J. Int., 111, 43-447.

Wan, T. and Q. Zhao (2012). The genesis of tectono-magmatism in eastern China, Sci China Earth Sci., 55, 347-354, doi: 10.1007/s11430-011-4361-4.

Wang, C., L. Chang, Z. Ding, Q. Liu, W. Liao and L. M. Flesch (2014). Upper mantle anisotropy and crust-mantle deformation pattern beneath the Chinese mainland, Sci. China Earth Sci., 57, 132-143.

Wang, C., L. M. Flesch, P. G. Silver, L. Chang and W. W. Chan (2008). Evidence for mechanically coupled lithosphere in Central Asia and resulting implications, Geology, 36, 5, 363-366.

Wang, C., X. Zhang, B. Chen, X. Chen, S. Song, J. Zheng, H. Hu and H. Lou (1997). Crustal structure of Dabieshan orogenic belt, Sci. China Earth Sci. (in Chinese), 40, 5, 456-462.

Wang, G., J. Teng and Z. Zhang (2000). The Continental Structure Pattern of South China and its Marginal Regions, Progress in Geophysics (in Chinese), 15, 3, 25-44.

Wang, Q., F. Niu, Y. Gao and Y. Chen (2016). Crustal structure and deformation beneath the NE margin of the Tibetan plateau constrained by teleseismic receiver function data, Geophys. J. Int., 204, 167-179.

Wu, J., Y. Gao, J. Cai, Y. Shi, S. Lin, T. Bao and Z. Li (2007). Preliminary study on seismic anisotropy in the crust in southeast of Cathaysia Block, Chinese J. Geophys. (in Chinese), 50, 6, 1748-1756.

Wu, P., C. Wang, Z. Ding, L. Chang and Z. Li (2012). Seismic anisotropy of upper mantle beneath the Dabie-Sulu and its adjacent areas, Chinese J. Geophys. (in Chinese), 55, 8, 2539-2550.

Xiao, W., Y. Zhou, Z. Yang and X. Zhao (2000). Multiple Rotation and Amalgamation Processes of Dabie-Tanlu-Sulu Orogen, Adv. Earth Sci. (in Chinese), 15, 2, 24-30.

Xiong, X., R. Gao, Q. Li, Z. Lu, H. Wang, W. Li and Y. Guan (2009). The Moho Depth of South China Revealed by Seismic Probing. Acta Geoscientica Sinica (in Chinese), 30, 6, 774-786.

Xu, X. and S. Gao (2015). The structure and formation of the Cenozoic fault basin in the lower Yangtze region, Earth Science Frontiers (in Chinese), 22, 6, 148-166.

Xu, X., S. O' Reilly, W. Griffin, X. Wang, N. Pearson and Z. He (2007). The crust of Cathaysia: Age, assembly and reworking of two terranes, Precambrian Research, 158, 51-78.

Xu, Y., Z. Li, T. Hao, J. Liu and J. Liu (2007). Pn Wave Velocity and Anisotropy in the Northeastern South China Sea and Adjacent Region, Chinese J. Geophys. (in Chinese), 50, 5, 1473-1479.

Yang, X., H. Li, Y. Li, Q. Lv, G. Zhang, G. Jiang and X. Li (2019). Seismic anisotropy beneath eastern China from shear wave splitting, Geophys. J. Int., 218, 3, 1642-1651.

Yang, Y., H. Yao, P. Zhang and L. Chen (2018). Crustal azimuthal anisotropy in the trans-North China orogen and adjacent regions from receiver functions, Sci. China Earth Sci., 61: 903-913.

Ye, Z., Q. Li, H. Zhang, J. Li and Q. Wu (2019). Crustal and uppermost mantle structure across the Lower Yangtze region and its implications for the late Mesozoic magmatism and metallogenesis, eastern South China, Phys. Earth Planet. Inter., 297, 106324.

Yu, D., Y. Wang, B. Yang and H. Wang (2016). Geochemical features of granites from two sides of the southern segment of the Tan-Lu fault zone: Evidence for middle-lower crust flow of the Dabie orogenic belt, Acta Petrologica Sinica, 32, 4,1001-1012.

Zandt, G. and C. Ammon (1995). Continental crust composition constrained by measurements of crustal Poisson's ratio, Nature, 374, 152-154.

Zhang, C., M. Santosh, Q. Zhu, X. Chen and W. Huang (2014). The Gondwana connection of South China: Evidence from monazite and zircon geochronology in the Cathaysia Block, Gondwana Res., 28, 3, 1137-1151.

Zhang, G., A. Guo, Y. Wang, S. Li, Y. Dong, S. Liu, D. He, S. Cheng, R. Lu and A. Yao (2013). Tectonics of South China Continent and its implications, Sci. China Earth Sci (in Chinese), 56, 1804-1828.

Zhang, Y., D. Shi, Q. Lü, Y. Xu, Z. Xu, X. Gong, J. Yan and T. Xu (2021a). A fine crustal structure and geodynamics revealed by receiver functions along the Guangchang-Putian line in the Cathaysia Block, South China, Tectonophysics, 815, 229007.

Zhang, Y., D. Shi, Q. Lü, Y. Xu, Z. Xu, J. Yan, C. Chen and T. Xu (2021b). The crustal thickness and composition in the eastern South China Block constrained by receiver functions: Implications for the geological setting and metallogenesis, Ore Geol. Rev., 130, 103988.

Zhao, L., T. Zheng, and G. Lu (2013). Distinct upper mantle deformation of cratons in response to subduction: Constraints from SKS wave splitting measurements in eastern China, Gondwana Res., 23, 1, 39-53.

Zhao, Y., Y., Duan, C. Zou, Y. Wei, Y. Qiu, J. Lin and X. Li (2015). Study of the receiver function profile from Jiujiang, Jiangxi Province to Ninghua, Fujian Province, Acta Seismologica Sinica, 37(5): 722-732.

Zheng, S., X. Sun, X. Song, Y. Yang and M. H. Ritzwoller (2008). Surface wave tomography of China from ambient seismicnoise correlation, Geochem. Geophys. Geosyst., 9, Q05020.

Zheng, T., Z. Ding, J. Ning, L. Chang, X. Wang, F. Kong, K. H. Liu and S. S. Gao (2018). Crustal azimuthal anisotropy beneath the southeastern Tibetan Plateau and its geodynamic implications, J. Geophys. Res., 123.

Zheng, T., Z. Ding, J. Ning, K. H. Liu, S. S. Gao, L. Chang, F. Kong and X. Fan (2019). Crustal azimuthal anisotropy beneath the central North China Craton revealed by receiver functions, Geochem. Geophys. Geosyst, 20, 2235-2251.

Zheng, Y., W. Xiao and G. Zhao (2013). Introduction to tectonics of China, Gondwana Res., 23, 1189-1206.

Zhou, X., and W. Li (2000). Origin of late mesozoic igneous rocks in southeastern China: implications for lithosphere subduction and underplating of mafic magmas, Tectonophysics, 326, 34, 269-287.
Zhou, X., T., Sun, W. Shen and L. Shu (2006). Petrogenesis of Mesozoic granitoids and volcanic rocks in South China: a response to tectonic evolution, Episodes, 29, 1, 26-33.
Zhu, L. and H. Kanamori (2000). Moho depth variation in southern California from teleseismic receiver functions, J. Geophys. Res., 105, 2969-2980.

***CORRESPONDING AUTHOR:** **Yuan GAO**,
Key Laboratory of Earthquake Prediction, Institute of Earthquake Forecasting,
China Earthquake Administration, Beijing, 100036, China
e-mail: gaoyuan@ief.ac.cn; qzgyseis@163.com